

## Aberystwyth University

### *Influence of bedrock mineral composition on microbial diversity in a subglacial environment*

Mitchell, Andrew Charles; Lafreniere, Melissa J.; Skidmore, Mark L.; Boyd, Eric S.

*Published in:*

Geology

*DOI:*

[10.1130/G34194.1](https://doi.org/10.1130/G34194.1)

*Publication date:*

2013

*Citation for published version (APA):*

Mitchell, A. C., Lafreniere, M. J., Skidmore, M. L., & Boyd, E. S. (2013). Influence of bedrock mineral composition on microbial diversity in a subglacial environment. *Geology*, 41(8), 855-858.  
<https://doi.org/10.1130/G34194.1>

#### **General rights**

Copyright and moral rights for the publications made accessible in the Aberystwyth Research Portal (the Institutional Repository) are retained by the authors and/or other copyright owners and it is a condition of accessing publications that users recognise and abide by the legal requirements associated with these rights.

- Users may download and print one copy of any publication from the Aberystwyth Research Portal for the purpose of private study or research.
- You may not further distribute the material or use it for any profit-making activity or commercial gain
- You may freely distribute the URL identifying the publication in the Aberystwyth Research Portal

#### **Take down policy**

If you believe that this document breaches copyright please contact us providing details, and we will remove access to the work immediately and investigate your claim.

tel: +44 1970 62 2400  
email: [is@aber.ac.uk](mailto:is@aber.ac.uk)

# Geology

## Influence of bedrock mineral composition on microbial diversity in a subglacial environment

--Manuscript Draft--

<b>Manuscript Number:</b>	G34194R1
<b>Full Title:</b>	Influence of bedrock mineral composition on microbial diversity in a subglacial environment
<b>Short Title:</b>	Mineralogical controls on microbial diversity in a subglacial environment
<b>Article Type:</b>	Article
<b>Keywords:</b>	Glacier, microbiology, mineralogy, pyrite, oxyhydroxides, climate, microbe-mineral interactions
<b>Corresponding Author:</b>	Andrew C. Mitchell, PhD Aberystwyth University Aberystwyth, Ceredigion UNITED KINGDOM
<b>Corresponding Author Secondary Information:</b>	
<b>Corresponding Author's Institution:</b>	Aberystwyth University
<b>Corresponding Author's Secondary Institution:</b>	
<b>First Author:</b>	Andrew C. Mitchell, PhD
<b>First Author Secondary Information:</b>	
<b>Order of Authors:</b>	Andrew C. Mitchell, PhD
	Melissa Lafrenière
	Mark L Skidmore
	Eric Boyd
<b>Order of Authors Secondary Information:</b>	
<b>Manuscript Region of Origin:</b>	CANADA
<b>Abstract:</b>	<p>Microorganisms in subglacial environments drive the chemical weathering of bedrock, however, the influence of bedrock mineralogy on the composition and activity of microbial assemblages in such environments is poorly understood. Here, using a combination of in situ mineral incubation and DNA fingerprinting techniques, we demonstrate that pyrite is the dominant mineralogical control on subglacial bacterial community structure and composition. In addition, we show that the abundance of Fe in the incubated minerals influences the development of mineral associated biomass. The ubiquitous nature of pyrite in many common bedrock types and high SO<sub>4</sub><sup>2-</sup> concentrations in most glacial meltwaters suggests that pyrite may be a dominant lithogenic control on microbial communities in many subglacial systems. Mineral-based energy may therefore serve a fundamental role in sustaining subglacial microbial populations and enabling their persistence over glacial-interglacial timescales.</p>
<b>Response to Reviewers:</b>	See attached cover letter

Cover letter

[Click here to download Cover letter: G34194\\_coverletter\\_Mitchell\\_mls.doc](#)

1 Influence of bedrock mineral composition on microbial  
2 diversity in a subglacial environment

3 Andrew C. Mitchell<sup>1,2</sup>, Melissa J. Lafrenière<sup>3</sup>, Mark. L. Skidmore<sup>4</sup>, and Eric S.  
4 Boyd<sup>5</sup>

5 <sup>1</sup>*Institute of Geography and Earth Sciences, Aberystwyth University, Aberystwyth, SY23*  
6 *3DB, UK*

7 <sup>2</sup>*Center for Biofilm Engineering, Montana State University, Bozeman, Montana 59717,*  
8 *USA*

9 <sup>3</sup>*Department of Geography, Queen's University, Kingston, Ontario K7L 3N6, Canada*

10 <sup>4</sup>*Department of Earth Sciences, Montana State University, Bozeman, Montana 59717,*  
11 *USA*

12 <sup>5</sup>*Department of Chemistry and Biochemistry, Montana State University, Bozeman,*  
13 *Montana 59717, USA*

14 **ABSTRACT**

15 Microorganisms in subglacial environments drive the chemical weathering of  
16 bedrock, however, the influence of bedrock mineralogy on the composition and activity  
17 of microbial assemblages in such environments is poorly understood. Here, using a  
18 combination of in situ mineral incubation and DNA fingerprinting techniques, we  
19 demonstrate that pyrite is the dominant mineralogical control on subglacial bacterial  
20 community structure and composition. In addition, we show that the abundance of Fe in  
21 the incubated minerals influences the development of mineral associated biomass. The  
22 ubiquitous nature of pyrite in many common bedrock types and high SO<sub>4</sub><sup>2-</sup> concentrations

in most glacial meltwaters suggests that pyrite may be a dominant lithogenic control on microbial communities in many subglacial systems. Mineral-based energy may therefore serve a fundamental role in sustaining subglacial microbial populations and enabling their persistence over glacial-interglacial timescales.

## INTRODUCTION

Terrestrial ice masses currently cover  $\sim 15 \times 10^6 \text{ km}^2$ , roughly 10% of Earth's land surface. The presence of viable microbes in terrestrial ice, subglacial sediments, and proglacial meltwaters has been demonstrated (Christner, 2002; Sharp et al., 1999; Skidmore et al., 2005; Skidmore et al., 2000) and *ex-situ* (Boyd et al., 2011; Christner, 2002) and *in situ* (Boyd et al., 2010) evidence of microbial activities has been presented. The lack of light energy capable of driving photosynthesis in subglacial environments suggests that energy for cellular synthesis and the maintenance of microorganisms is supplied from chemical energy (chemosynthesis), likely derived from weathering of the local bedrock (e.g., minerals) (Luttge et al., 2005; Shock, 2009). Indeed, numerous lines of evidence suggest that many geochemical processes, including mineral weathering and redox transformations in subglacial environments, are driven by microorganisms (Boyd et al., 2011; Hamilton et al., 2013; Montross et al., 2013; Skidmore et al., 2005; Wadham et al., 2004; Wynn et al., 2007). Hydrological regimes (Tranter et al., 2005), nutrient availability and redox conditions (Wadham et al., 2004; Wynn et al., 2007) have been shown to impact the function of microorganisms in subglacial environments. However, the influence of bedrock mineralogy on the structure, composition and activity of microbial assemblages in subglacial systems remains poorly understood despite its

potential importance over a significant portion of Earth's surface both today and on  
glacial-interglacial time scales.

The importance of pyrite ( $\text{FeS}_2$ ) oxidation as a dominant geochemical process in  
subglacial environments has been documented (Bottrell and Tranter, 2002; Brown, 2002;  
Tranter et al., 2002), and more recent evidence suggests that this process is microbially  
mediated (Montross et al., 2013; Skidmore et al., 2005; Wadham et al., 2004). Sulfate is  
the second most dominant anion (after bicarbonate) in most proglacial and subglacial  
meltwaters from alpine, arctic and antarctic environments (Brown, 2002), and  
concentrations of  $\text{SO}_4^{2-}$  are always significantly enriched relative to possible input waters  
(e.g., ice- or snow-melt), indicating a lithogenic source. In addition to  $\text{SO}_4^{2-}$ , other  
products of pyrite weathering are often ubiquitous in glacial meltwaters and sediments  
(Mitchell et al., 2001), including nano particles of Fe-oxyhydroxides (Raiswell et al.,  
2009). Equally, surveys of subglacial microbial community 16S rRNA transcripts  
(Hamilton et al., 2013) and genes (Lanoil et al., 2009; Skidmore et al., 2005) often yield  
sequences that are closely affiliated with organisms that actively metabolize Fe, S, and/or  
FeS minerals. Therefore, while geochemical and microbiological evidence suggests Fe  
and S cycling are important in subglacial systems, the extent to which lithology and  
mineralogy shape community structure, composition, and activity is unknown. Here we  
employ a method to isolate the influence of mineralogy on the composition and structure  
of microbial communities in the subglacial environment at Robertson Glacier (RG),  
Alberta, Canada (115°20'W, 50°44'N; Item DR1 and Fig. DR1a in the GSA Data  
Repository<sup>1</sup>). This approach employs coupon samplers composed of capped stainless-  
steel mesh cylinders (Item DR1 and Fig. DR1b) that compartmentalize different minerals

during in situ incubation (Boyd et al., 2007) in the glacial outflow channel of RG ~10 m downstream of the glacier terminus, in order to assess the influence of mineralogy on the structure, composition, and abundance of the microbial community.

## **MATERIALS AND METHODS**

Combustion-sterilized rocks and minerals (1.4–1.7 mm diameter) were incubated in the glacial meltwater stream at RG (RW [western drainage]) for 7 mo. over winter in order to promote colonization of mineral substrata contained in pre-sterilized coupon samplers by microorganisms that originated from the subglacial system (Item DR1 and Fig. DR1b). The close proximity of the coupons to the glacier and the subglacial source for the waters passing through the coupons provide confidence that the microbial colonization that occurred reflects subglacial microbial diversity. The selection of minerals, derived from mineral collections and chemically characterized by energy-dispersive X-ray spectroscopy (EDS) and X-ray diffraction (XRD) (Item DR1), included those that could serve as electron donors or acceptors (pyrite,  $[\text{Fe}^{2+}, \text{S}^-]$ , hematite and magnetite  $[\text{Fe}^{3+}]$ ) and olivine  $[\text{Fe}^{2+}]$  (90% forsterite + 10% fayalite;  $\text{Fo}_{90}\text{Fa}_{10} = \text{Mg}_{1.8}\text{Fe}_{0.2}\text{SiO}_4$ ;  $\text{Fe}^{2+} = 75,000 \pm 1425$  ppm [Item DR1 and Table DR1]). Minerals that offered no obvious metabolic substrate [quartz ( $\text{SiO}_2$ ), calcite ( $\text{CaCO}_3$ )] but were abundant in catchment bedrock (Table DR1; Sharp et al., 2002) were also included. In addition, we included representative rock from the RG catchment (dark shale containing quartz, microcline, calcite, and pyrite) which was prepared in the same way as the pure mineral phases. RG rock contained  $9800 \pm 764$  ppm  $\text{Fe}^{2+}$  and  $3000 \pm 360$  ppm S, and assuming all S came from pyrite, an estimated pyrite content of 0.56 weight % (Table DR1). Subglacial (RG water) and supraglacial meltwaters were collected aseptically and

91 filtered through sterilized filter apparatus with 0.22  $\mu\text{m}$  pore size polyvinylidene  
92 difluoride membrane at the time of coupon deployment to compare the native community  
93 with that which developed on the coupon minerals. Fine-grained subglacial sediment was  
94 also collected aseptically (RG sediment) from the site of coupon deployment at the time  
95 the coupon was retrieved. All mineral and sediment samples were immediately flash  
96 frozen on site using dry ice (Item DR1).

97 Coupon minerals, subglacial sediments (RG sediment), and filters with subglacial  
98 suspended sediments and planktonic (e.g., suspended) cells (RG water) were subjected to  
99 community DNA extraction, polymerase chain reaction (PCR) amplification, and  
100 bacterial 16S rRNA gene terminal-restriction length polymorphism (T-RFLP) (Item  
101 DR1). Distinct T-RFs were considered to be unique operational taxonomic units and were  
102 the unit by which individual phylotypes were demarcated. Comparison of T-RFLP  
103 profiles was performed using the Bray-Curtis index, which represents an abundance  
104 weighted metric describing the similarity of communities (Item DR1). Clone library  
105 construction was also performed on pyrite- and RG-sediment associated communities, as  
106 previously described (Boyd et al., 2007), to determine similarity with known  
107 microorganisms (Item DR1). Filtered waters (0.22  $\mu\text{m}$ ) were immediately measured for  
108 pH and electrical conductivity in the field, and were analyzed for major anions, cations,  
109  $\delta^{34}\text{S-SO}_4^{2-}$ ,  $\delta^{18}\text{O-SO}_4^{2-}$ , and  $\delta^{18}\text{O-H}_2\text{O}$  (Item DR1).

## 110 **RESULTS AND DISCUSSION**

### 111 **Geochemical Evidence of Mineral Weathering**

112 Enrichment of sulfate ( $\text{SO}_4^{2-}$ ) in subglacial waters, relative to supraglacial waters,  
113 indicates pyrite weathering in the subglacial environment of RG (Table DR2 and Item



DR2). The  $\delta^{34}\text{S}\text{-SO}_4^{2-}$  and  $\delta^{18}\text{O}\text{-SO}_4^{2-}$  values in meltwaters also indicate pyrite oxidation (Table DR2 and Item DR2). Our results are consistent with previous geochemical (Sharp et al., 1999; Tranter et al., 2002) and isotopic studies (Bottrell and Tranter, 2002; Wadham et al., 2004) of other glacial catchments, which indicate a role for pyrite weathering in solute liberation, which has been argued to be the result of microbial activity. If microorganisms are driving pyrite weathering in RG subglacial sediments, then the microbial community would be expected to harbor 16S rRNA genes affiliated with organisms capable of this physiological activity. Indeed, examination of microbial communities from RG (Hamilton et al., 2013) and from glacial catchments with similar geology to that of RG (Skidmore et al., 2005) reveal the presence of sequences affiliated with several organisms capable of oxidizing Fe and/or S.

#### **RG Subglacial Sediment Microbial Community Composition**

The majority of 16S rRNA genes recovered from sediments sampled adjacent to the mineral coupon incubation site (Fig. 1; Table DR3, RG sediment), exhibited close affiliation with  $\beta$ - and  $\gamma$ -proteobacteria (e.g., *Thiobacillus* spp. [ $>94\%$  identity], *Acidithiobacillus ferrooxidans* [90% identity], and *Siderooxidans lithoautotrophicus* [96% identity]). These organisms have been demonstrated to catalyze the oxidation of soluble and/or solid phase ferrous iron and sulfur in pure cultures (Karavaiko et al., 2003; Okereke and Stevens, 1991; Suzuki et al., 1990; Item DR2). Indeed,  $\beta$ - and  $\gamma$ -Proteobacteria are the dominant phylogenetic groups in nearly all subglacial systems investigated from alpine and polar environments (e.g., Foght et al., 2004; Skidmore et al., 2005) and all of these glaciers are underlain by bedrock that contains pyrite, similar to the bedrock at RG. Collectively, these observations suggest that pyrite weathering is an

important process and is likely an important determinant in structuring the composition of microbial communities in this and other subglacial systems.

### **Mineralogical Controls on Community Structure and Composition**

In order to further examine the role of pyrite and other minerals in structuring the composition of bacterial communities in the subglacial system, we compared 16S rRNA gene T-RFLP profiles (each T-RF considered a unique taxonomic unit) of bacterial communities associated with the coupon incubated mineral surfaces to those associated with native sediments (RG sediment) using the Bray Curtis (BC) similarity index.

Importantly, such in situ experiments represent a discrete colonization interval (7 mo.) and the observations from such minerals may be confounded by differences in microbial colonization and successional dynamics. Notwithstanding, the bacterial community that associates with the RG subglacial sediment is most similar to that associated with pyrite (BC index = 0.40) (Fig. 2, Tables DR4 and DR5), adding further evidence that supports the influence of pyrite on the composition and structure of bacterial communities in the subglacial environment at RG. The RG sediment bacterial community was also similar to the communities that associated with the native rock from the RG catchment that was also incubated in the subglacial coupons, RG Rock (BC index = 0.37). For example, the RG sediment-associated bacterial community shared seven dominant phylotypes with the RG rock- and pyrite-associated communities. Together these phylotypes accounted for 37.6% of the RG sediment-associated community, 70.9% of RG rock-associated community, and 53.4% of the pyrite-associated community (Table DR4). Interestingly, the communities that associated with pyrite, RG rock, and RG sediment formed a cluster along with the community from RG water (subglacial meltwater containing suspended

sediment and planktonic cells) associated community (Fig. 2), further evincing the compositional similarity of these communities to each other. These results, which demonstrate the similarity of communities on pyrite with those associated with native sediments, rocks and water, are supported by sequence-based comparisons of community 16S rRNA genes which also reveal significant overlap in the phylogenetic composition of pyrite- and RG sediment-associated communities (Table DR3). Because pyrite is a constituent of RG rock (0.56 wt%), RG sediment (1.2 wt% [Table DR1]), and thus the suspended sediment in the RG water, these collective observations strongly suggest that pyrite, even in low concentrations, is a key control on the subglacial sediment-associated bacterial communities, perhaps due to a selective advantage to organisms that actively metabolize Fe and S in this mineral.

The other Fe-bearing minerals, hematite and magnetite, harbored microbial communities similar in structure and composition to each other (BC index = 0.42), which would be expected considering that they are both Fe-oxides. Importantly, the bacterial communities associated with hematite and magnetite were also similar to the communities associated with the RG sediment (BC index = 0.26 and 0.34, respectively), though less than when compared with the pyrite associated community (BC index = 0.40) (Fig. 2; Table DR5). While XRD was unable to detect Fe-oxides in the RG bedrock (Table DR2), Fe-oxyhydroxides, which are derived from the oxidation of pyrite (e.g., Tranter et al., 2002), are likely to be present in the subglacial RG sediments. Moreover, direct measurements in other glacial environments indicate Fe-oxyhydroxides exist as single grain or aggregate nano-particles and/or as labile surface coatings of other mainly silicate sediments (Mitchell et al., 2001; Raiswell et al., 2009). Thus Fe-oxyhydroxides in

RG sediments may also influence microbial communities in subglacial environments, and account for the high similarity of hematite and magnetite communities with RG sediment communities. This hypothesis is further supported by the recovery of 16S rRNA gene clones from the RG sediment-associated library that are affiliated with *Rhodoferrum* *ferrireducens* (Table DR3), an iron reducing chemotroph (Finneran et al., 2003). Olivine, while containing Fe<sup>2+</sup> at 7.5 wt% (Table DR2) harbored communities that shared little resemblance to RG rock and RG sediment communities, presumably because it was not detected in the catchment bedrock.

Communities associated with quartz and calcite exhibited low similarity with, and that were distinct from those which associated with RG sediment, RG water and RG rock (Fig. 2) despite their abundance in the catchment bedrock (Table DR1). This is presumably due to a lack of any potential metabolic substrate associated with the calcite or quartz mineral phases, aside from the potential use of calcite derived carbonate as a source of carbon. Therefore T-RFLP add further evidence suggesting that Fe and S containing minerals, particularly pyrite, strongly influence the structure and composition of subglacial bacterial communities presumably due the selective advantage afforded to those that metabolize these available substrates.

#### **Mineralogical Controls on Biomass**

We compared the quantity of genomic DNA extracted from the mineral phases as a proxy for assessing the amount of biomass that accumulated on the mineral surfaces, with the premise that higher biomass loadings might indicate that the populations are using the minerals as a substrate to support their metabolism. We hypothesized that minerals containing Fe and S, which can support the metabolism of a wide variety of

microbial populations (Luttge et al., 2005; Shock, 2009), would harbor a higher biomass. Surface associated biomass was particularly pronounced on Fe bearing oxides and sulfides (hematite, magnetite, and pyrite; 204, 190, and 83 ng DNA/g mineral, respectively), but much lower on pyrite containing RG rock and Fe-bearing olivine [Fo<sub>90</sub>Fa<sub>10</sub>] (25 and 17 ng DNA/g mineral, respectively) (Fig. 3). These differences are correlated with the abundance of Fe in the minerals and rocks, which was greatest in hematite (70 wt%), magnetite (84 wt%) and pyrite (47 wt%), compared to only 7.5 wt% in olivine and 1.6 wt% in RG rock. The lowest surface-associated biomass was recovered from calcite and quartz (17 and 16 ng DNA/g mineral, respectively), which may reflect the lack of any Fe or other abundant metabolic substrate in these carbonate and silicate minerals (Fig. 3).

These data demonstrate that the abundance of Fe in subglacial minerals influences the respective surface-associated biomass, suggesting that these populations are using Fe in the minerals to support their metabolism. Importantly, the valence state of Fe in these minerals is different (pyrite 2<sup>-</sup>, hematite 3<sup>+</sup>, magnetite 2<sup>+</sup>/3<sup>+</sup>), consistent with community 16S rRNA gene compositions, which indicate the presence of populations putatively involved in Fe oxidation or reduction in the RG sediments (Table DR3). Similarly, the metabolism of S in pyrite is also likely to have a strong influence on surface associated biomass, as evinced by pyrite associated 16S rRNA gene sequences with a high similarity to microorganisms known to metabolize sulfur (Table DR3), but this cannot be comparatively quantified in the minerals used. Together with molecular-based data that indicate that pyrite and Fe-oxides harbor communities that are most similar to the RG sediments, this strongly suggests that (1) pyrite and its weathering products (i.e., Fe

oxyhydroxides, thiosulfate) strongly influence subglacial microbial communities due to their ability to transform and utilize the mineral phase through redox reactions, and (2) the Fe concentration of Fe bearing minerals and rocks has a direct influence on surface-associated biomass in subglacial environments. Microbial interaction with mineral surfaces and the metabolism of key species such as Fe and S may therefore be a critical mechanism for sustaining life in subglacial systems at present, and over glacial-interglacial time scales. This is of global significance given that ice sheets covered 30% of Earth's continental land surface during Quaternary glaciations, and up to 100% during pervasive low latitude glaciations in the Neoproterozoic (Kirschvink, 1992).

## CONCLUSION

Previous studies have demonstrated the importance of particulate-associated microbes in subglacial environments and indicate that this biomass represents a larger fraction of the community when compared with planktonic populations (e.g. Sharp et al., 1999; Skidmore et al., 2005). Our results indicate that mineralogy, due to the influence on community composition, structure, and abundance may help to explain these previous observations. Specifically, pyrite is the dominant mineralogical control on subglacial community structure at RG, and mineral associated biomass was proportional to the abundance of Fe in the incubated minerals. This suggests the importance of Fe and S metabolism at the mineral surface, as supported by the recovery of 16S rRNA gene sequences which were closely affiliated with organisms that are known to metabolize these species. Solid phase mineral utilization by microbial populations is likely a critical, life-sustaining strategy that enables subglacial ecosystems to persist during extended

glacial-interglacial time scales when ice masses have covered between 30% and 100% of Earth's continental land surface.

## ACKNOWLEDGMENTS

Mitchell and Boyd were supported by a grant from the NASA Montana Space Grant Consortium (MSGC). Boyd acknowledges support from the NASA Astrobiology Institute (NAI) postdoctoral fellowship program. Boyd and Skidmore were supported by NASA Exobiology and Evolutionary Biology Program through grant NNX10AT31G. EDX analysis was performed by Vernon Phoenix, University of Glasgow. We thank Dave Mogk for providing mineral specimens from the MSU mineral collection.

## REFERENCES CITED

- Bottrell, S.H., and Tranter, M., 2002, Sulphide oxidation under partially anoxic conditions at the bed of the Haut Glacier d'Arolla, Switzerland: Hydrological Processes, v. 16, p. 2363–2368, doi:10.1002/hyp.1012.
- Boyd, E., Cummings, D., and Geesey, G., 2007, Mineralogy influences structure and diversity of bacterial communities associated with geological substrata in a pristine aquifer: Microbial Ecology, v. 54, p. 170–182, doi:10.1007/s00248-006-9187-9.
- Boyd, E.S., Skidmore, M., Mitchell, A.C., Bakermans, C., and Peters, J.W., 2010, Methanogenesis in subglacial sediments: Environmental Microbiology Reports, v. 2, p. 685–692, doi:10.1111/j.1758-2229.2010.00162.x.
- Boyd, E.S., Lange, R.K., Mitchell, A.C., Havig, J.R., Hamilton, T.L., Lafrenière, M.J., Shock, E.L., Peters, J.W., and Skidmore, M., 2011, Diversity, abundance, and potential activity of nitrifying and nitrate-reducing microbial assemblages in a

- 274 subglacial ecosystem: *Applied and Environmental Microbiology*, v. 77, p. 4778–  
275 4787, doi:10.1128/AEM.00376-11.
- 276 Brown, G.H., 2002, Glacier meltwater hydrochemistry: *Applied Geochemistry*, v. 17,  
277 p. 855–883, doi:10.1016/S0883-2927(01)00123-8.
- 278 Christner, B.C., 2002, Incorporation of DNA and protein precursors into macromolecules  
279 by bacteria at –15°C: *Applied and Environmental Microbiology*, v. 68, p. 6435–  
280 6438, doi:10.1128/AEM.68.12.6435-6438.2002.
- 281 Finneran, K.T., Johnsen, C.V., and Lovley, D.R., 2003, *Rhodoferrax ferrireducens* sp.  
282 nov., a psychrotolerant, facultatively anaerobic bacterium that oxidizes acetate with  
283 the reduction of Fe(III): *International Journal of Systematic and Evolutionary*  
284 *Microbiology*, v. 53, p. 669–673, doi:10.1099/ijs.0.02298-0.
- 285 Foght, J., Aislabie, J., Turner, S., Brown, C.E., Ryburn, J., Saul, D.J., and Lawson, W.,  
286 2004, Culturable bacteria in subglacial sediments and ice from two southern  
287 hemisphere glaciers: *Microbial Ecology*, v. 47, p. 329–340, doi:10.1007/s00248-003-  
288 1036-5.
- 289 Hamilton, T., Peters, J., Skidmore, M., and Boyd, E., 2013, Molecular evidence for an  
290 active endogenous microbiome beneath glacial ice: *ISME Journal*, v. 7 (in press).
- 291 Karavaiko, G.I., Turova, T.P., Kondrat'eva, T.F., Lysenko, A.M., Kolganova, T.V.,  
292 Ageeva, S.N., Muntyan, L.N., and Pivovarova, T.A., 2003, Phylogenetic  
293 heterogeneity of the species *Acidithiobacillus ferrooxidans*: *International Journal of*  
294 *Systematic and Evolutionary Microbiology*, v. 53, p. 113–119,  
295 doi:10.1099/ijs.0.02319-0.



- 296 Kirschvink, J.L., 1992, Late Proterozoic low-latitude global glaciation: The snowball  
297 earth, *in* Schopf, J.W., et al., eds., *The Proterozoic Biosphere: A Multidisciplinary*  
298 *Study*: Cambridge, UK, Cambridge University Press, p. 51–52.
- 299 Lanoil, B., Skidmore, M., Priscu, J.C., Han, S., Foo, W., Vogel, S.W., Tulaczyk, S., and  
300 Engelhardt, H., 2009, Bacteria beneath the West Antarctic Ice Sheet: *Environmental*  
301 *Microbiology*, v. 11, p. 609–615, doi:10.1111/j.1462-2920.2008.01831.x.
- 302 Luttge, A., Zhang, L., and Nealson, K.H., 2005, Mineral surfaces and their implications  
303 for microbial attachment: Results from Monte Carlo simulations and direct surface  
304 observations: *American Journal of Science*, v. 305, p. 766–790,  
305 doi:10.2475/ajs.305.6-8.766.
- 306 Mitchell, A., Brown, G.H., and Fuge, R., 2001, Minor and trace element export from a  
307 glacierized Alpine headwater catchment (Haut Glacier d’Arolla, Switzerland):  
308 *Hydrological Processes*, v. 15, p. 3499–3524, doi:10.1002/hyp.1041.
- 309 Montross, S.N., Skidmore, M., Tranter, M., Kivimäki, A.-L., and Parkes, R.J., 2013, A  
310 microbial driver of chemical weathering in glaciated systems: *Geology*, v. 41,  
311 p. 215–218, doi:10.1130/G33572.1.
- 312 Okereke, A., and Stevens, S.E., Jr., 1991, Kinetics of iron oxidation by thiobacillus  
313 ferrooxidans: *Applied and Environmental Microbiology*, v. 57, p. 1052–1056.
- 314 Raiswell, R., Benning, L.G., Davidson, L., Tranter, M., and Tulaczyk, S., 2009,  
315 Schwertmannite in wet, acid, and oxic microenvironments beneath polar and  
316 polythermal glaciers: *Geology*, v. 37, p. 431–434, doi:10.1130/G25350A.1.
- 317 Sharp, M., Parkes, J., Cragg, B., Fairchild, I.J., Lamb, H., and Tranter, M., 1999,  
318 Widespread bacterial populations at glacier beds and their relationship to rock

- 319 weathering and carbon cycling: *Geology*, v. 27, p. 107–110, doi:10.1130/0091-  
320 7613(1999)027<0107:WBPAGB>2.3.CO;2.
- 321 Sharp, M., Creaser, R.A., and Skidmore, M., 2002, Strontium isotope composition of  
322 runoff from a glaciated carbonate terrain: *Geochimica et Cosmochimica Acta*, v. 66,  
323 p. 595–614.
- 324 Shock, E.L., 2009, Minerals as energy sources for microorganisms: *Economic Geology*  
325 and the *Bulletin of the Society of Economic Geologists*, v. 104, p. 1235–1248,  
326 doi:10.2113/gsecongeo.104.8.1235.
- 327 Skidmore, M., Anderson, S.P., Sharp, M., Foght, J., and Lanoil, B.D., 2005, Comparison  
328 of microbial community compositions of two subglacial environments reveals a  
329 possible role for microbes in chemical weathering processes: *Applied and*  
330 *Environmental Microbiology*, v. 71, p. 6986–6997, doi:10.1128/AEM.71.11.6986-  
331 6997.2005.
- 332 Skidmore, M.L., Foght, J.M., and Sharp, M.J., 2000, Microbial life beneath a high arctic  
333 glacier: *Applied and Environmental Microbiology*, v. 66, p. 3214–3220,  
334 doi:10.1128/AEM.66.8.3214-3220.2000.
- 335 Suzuki, I., Takeuchi, T.L., Yuthasastrakosol, T.D., and Oh, J.K., 1990, Ferrous iron and  
336 sulfur oxidation and ferric iron reduction activities of *thiobacillus ferrooxidans* are  
337 affected by growth on ferrous iron, sulfur, or a sulfide ore: *Applied and*  
338 *Environmental Microbiology*, v. 56, p. 1620–1626.
- 339 Tranter, M., Sharp, M.J., Lamb, H.R., Brown, G.H., Hubbard, B.P., and Willis, I.C.,  
340 2002, Geochemical weathering at the bed of Haut Glacier d’Arolla, Switzerland—A  
341 new model: *Hydrological Processes*, v. 16, p. 959–993, doi:10.1002/hyp.309.

Tranter, M., Skidmore, M., and Wadham, J., 2005, Hydrological controls on microbial communities in subglacial environments: *Hydrological Processes*, v. 19, p. 995–998, doi:10.1002/hyp.5854.

Wadham, J.L., Bottrell, S., Tranter, M., and Raiswell, R., 2004, Stable isotope evidence for microbial sulphate reduction at the bed of a polythermal high Arctic glacier: *Earth and Planetary Science Letters*, v. 219, p. 341–355, doi:10.1016/S0012-821X(03)00683-6.

Wynn, P.M., Hodson, A.J., Heaton, T.H.E., and Chenery, S.R., 2007, Nitrate production beneath a High Arctic glacier, Svalbard: *Chemical Geology*, v. 244, p. 88–102, doi:10.1016/j.chemgeo.2007.06.008.

## FIGURE CAPTIONS

Figure 1. Phylogenetic affiliation of bacterial 16S rRNA genes in clone libraries generated from DNA extracted from pyrite (A) and Robertson Glacier (RG) sediment (B).

Figure 2. Hierarchical agglomerative clustering dendrogram depicting Bray–Curtis similarity of bacterial 16S rRNA gene assemblages (Table DR4 [see footnote 1]) associated with mineral substrata, Robertson Glacier (RG) sediments, or RG meltwater. Data transformed to dendrogram using the Ward distance method. P-values supporting clustering at each node are depicted.

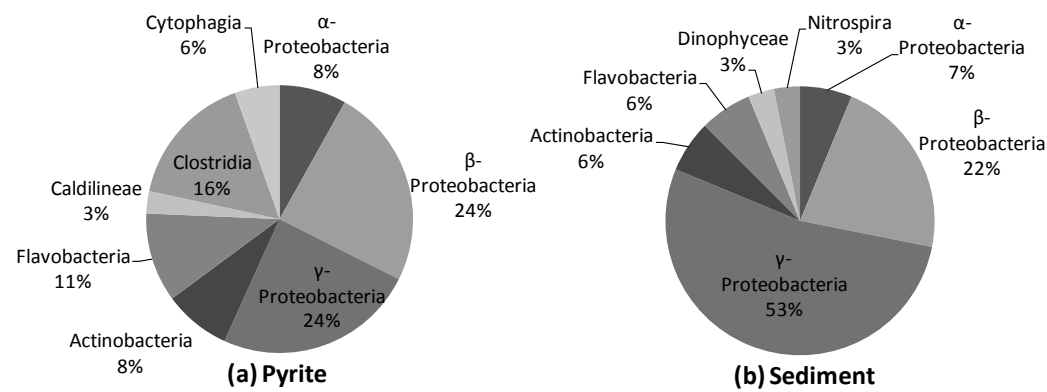
Figure 3. A: Biomass (extractable DNA as a proxy) associated with mineral substrata following 7 mo. colonization in subglacial stream. Error bars reflect standard deviation of

365 three replicate determinations of DNA concentration from a pool of three replicate  
366 mineral extractions. B: Correlation between biomass and Fe content, as determined by  
367 EDS (olivine, RG Rock, calcite and quartz; error bars smaller than symbols) or from pure  
368 phase stoichiometry (pyrite, hematite, and magnetite).

369

370 <sup>1</sup>GSA Data Repository item 2013xxx, xxxxxxxx, is available online at  
371 [www.geosociety.org/pubs/ft2013.htm](http://www.geosociety.org/pubs/ft2013.htm), or on request from [editing@geosociety.org](mailto:editing@geosociety.org) or  
372 Documents Secretary, GSA, P.O. Box 9140, Boulder, CO 80301, USA.

Figure 1.



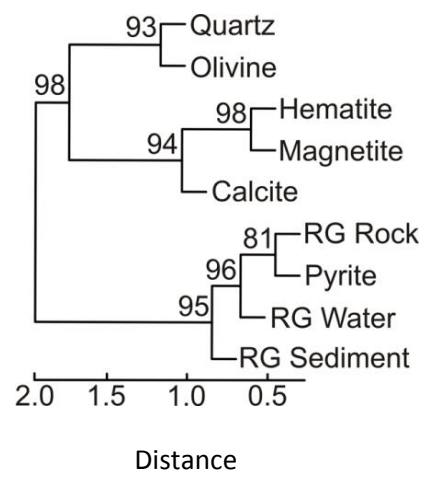


Figure 2.

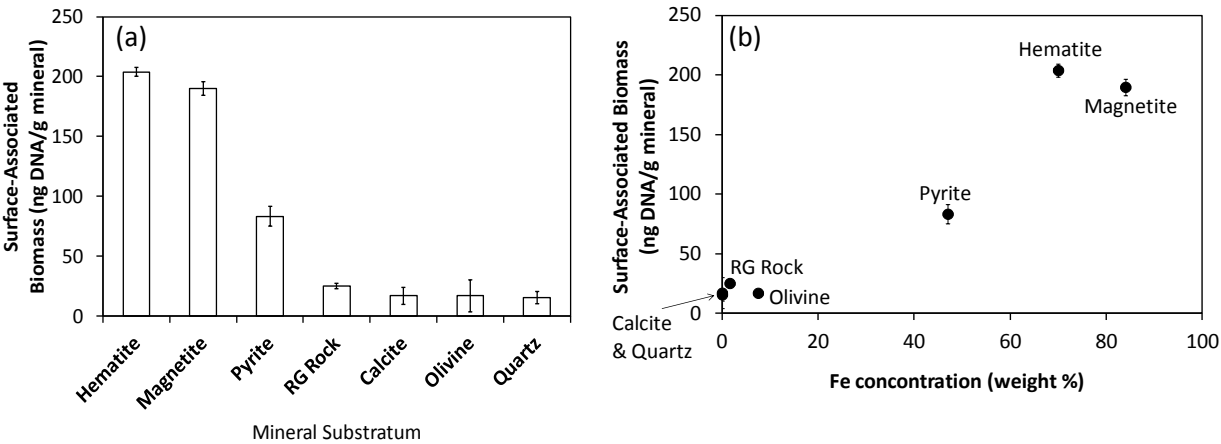


Figure 3.

**Supplemental Information. Data Repository.**

# **Influence of bedrock mineral composition on microbial diversity in a subglacial environment**

Andrew C. Mitchell<sup>1,2</sup>, Melissa J. Lafrenière<sup>3</sup>, Mark. L. Skidmore<sup>4</sup>,  
and Eric S. Boyd<sup>5</sup>.

<sup>1</sup> Institute of Geography and Earth Sciences, Aberystwyth University, Wales, UK, <sup>2</sup> Center for Biofilm Engineering, Montana State University, Bozeman, MT. USA, <sup>3</sup> Department of Geography, Queen's University, Kingston, ON, Canada, <sup>4</sup>Department of Earth Sciences, Montana State University, Bozeman, MT. USA, <sup>5</sup> Department of Chemistry and Biochemistry, Montana State University, Bozeman, MT. USA.



## **DR 1. DETAILED METHODS**

**DR 1.1. Field site description, sample collection and geology.** A detailed description of the hydrology and geology for Robertson Glacier (RG) has been previously reported (Sharp et al., 2002). Briefly, RG (115°20'W, 50°44'N) is a north facing valley glacier in Peter Lougheed Provincial Park, Kananaskis Country, Alberta, Canada. RG is approximately 2 km long, spans an elevation range from 2370 to 2900 m, and currently terminates on a flat till plain, although glacially smoothed bedrock surfaces are exposed along the glacier margins. Two principal subglacial meltwater streams (referred to here as RE [eastern drainage] and RW [western drainage]) drain from beneath the ice front (Fig. DR1a). The local bedrock is Upper Devonian in age (Mount Hawk, Palliser and Sassenach Formations) and consists of impure limestones, dolostones, and dolomitic limestones, with interbeds of shale, siltstone, and sandstone (McMechan, 1988).

**DR 1.2. Rock / Mineral substrata and coupon preparation and incubation.** Pyrite ( $\text{FeS}_2$ ), hematite ( $\text{Fe}_2\text{O}_3$ ), magnetite ( $\text{Fe}_3\text{O}_4$ ), quartz ( $\text{SiO}_2$ ), calcite ( $\text{CaCO}_3$ ), and olivine (90% Forsterite + 10% Fayalite;  $\text{Fo}_{90}\text{Fa}_{10} = \text{Mg}_{1.8}\text{Fe}_{0.2}\text{SiO}_4$  [Table DR1]) were obtained from WARD's Natural Science or the mineralogical collection at the Department of Earth Sciences, Montana State University. Minerals were crushed and sieved to obtain a near uniform particle size of 1.4-1.7 mm diameter. Only particles in the 1.4-1.7 mm diameter size range were retained for use in loading biofilm coupons in an attempt to minimize differences in particle surface area.

In addition, representative rocks were collected from outcrops on the valley sides and moraines in the RG catchment. These consisted of various impure limestones (argillaceous and silty limestone) and shales, which are the predominant lithologies (McMechan, 1988). Five of these (R1 to R5) representing the range of rocks present, were analyzed by powder X-

Ray Diffraction (XRD) to determine the mineralogical composition (Table DR1). These rocks, as well as the coupon minerals were analyzed by Energy-dispersive X-ray spectroscopy (EDS) to determine elemental composition by weight. Samples were powdered and analyzed in variable pressure (VP) mode and against measured standards. All of the catchment rocks analyzed were found to contain quartz, calcite, and one or more aluminosilicate minerals (microcline, montmorillonite, muscovite, nontronite, sanidine) as determined by XRD (Table DR1). Pyrite was present in three of the rocks (R1 [Silty Limestone], R3 [Shale] and R5 [Shale]). R5, a dark shale containing quartz, microcline, calcite and pyrite) was crushed and prepared in the same way as the pure mineral phases for use in the coupon sampler (RG Rock, Table DR1). The pyrite content of RG rock and RG Sediment was estimated at 0.56 and 1.2 weight % respectively, assuming all S came from pyrite, which is valid given the apparent lack of any other S sources from XRD of the catchment rocks. The mineralogy of the rocks suggests that the major elements and their ions capable of serving as a substrate to support microbial metabolism in the catchment rocks were  $\text{Fe}^{2+}$  and  $\text{S}^-$  from pyrite ( $\text{FeS}_2$ ), since this was present in 3 of the 5 rocks analysed. While Fe containing nontronite ( $\text{Na}_{0.3}\text{Fe}_2\text{Si}_4\text{O}_{10}(\text{OH})_24\text{H}_2\text{O}$ ), and ankerite ( $\text{Ca}(\text{Fe,Mg})(\text{CO}_3)_2$ ) were detected, these were only present in one of the five rocks. Olivine stoichiometry was determined from EDS results (Table DR1).

Mineral coupons, composed of capped stainless steel mesh cylinders (25.4 x 1.27 cm; 1-mm mesh size) (Figure DR1b), were prepared with approximately 5 g each of pyrite, hematite, magnetite, quartz, calcite, olivine [ $\text{Fo}_{90}\text{Fa}_{10} = \text{Mg}_{1.8}\text{Fe}_{0.2}\text{SiO}_4$ ], and RG Rock. All substrata were separated within the coupon by plugs of glass wool. Mineral-loaded coupons were sterilized by combustion (550°C, 6 h) under an atmosphere of  $\text{N}_2$ . Coupons were suspended in the glacial outflow channel of RW approximately 10 meters downstream of the

glacier terminus where the stream bed was well developed. Coupons were incubated for seven months, spanning October 2007 to July 2008 in order to promote colonization of substrata by those microorganisms with a propensity for attachment. The large coupon mesh size allowed access of the particle surfaces to bacteria suspended in the surrounding groundwater. After incubation, coupons were retrieved, placed in sterile bags, frozen on site using a dry ice/ethanol slurry, and transported frozen to Montana State University where they were stored at -80°C until further processed.

**DR 1.3. Subglacial Meltwater and Sediment Sampling and Processing.** All sample collection and processing was undertaken using aseptic techniques, as described below. Subglacial meltwaters were collected from RW at the site of coupon deployment during the summer ablation season (July 2007) and at the time that the coupon was deployed (October, 2007). Supraglacial meltwaters, from the surface of the glacier, were also collected during July 2007. Samples of subglacial meltwaters (RW water) were collected in autoclaved sterile bottles and approximately 500 mL was immediately filtered in an autoclaved Nalgene filter unit containing pre-sterilized 0.22 µm PVDF membrane filters that were emplaced using ethanol soaked, flame sterilized metal tweezers. Following filtration, the filters with accumulated suspended sediment were placed in sterile DNA free 2.0 mL screw-cap vials using ethanol soaked, flame sterilized metal tweezers and were immediately frozen using a dry ice/ethanol slurry. Samples were transported back to MSU frozen where they were stored at -80°C until processed for genomic DNA extraction. In the laboratory, filters were cut in half using a sterile spatula and were placed in separate bead beating tubes for genomic DNA extraction (see below). 500 mg aliquots of fine-grained subglacial sediment (RG Sediment) were also collected from the site of coupon deployment at the time that the coupon was retrieved using ethanol soaked, flame sterilized metal scoops. Triplicate subsamples of

sediment were placed in sterile bead beating tubes in the field with sterile spatulas and tubes and contents were immediately flash frozen on site in a dry ice/ethanol slurry. Sediment samples were kept at -80°C until further processed for genomic DNA extraction.

**DR 1.4. Mineral Substrata Processing.** Mineral coupons were thawed and disassembled in a sterile laminar flow hood. Each individual mineral phase was removed from the coupon and granules were placed in a sterile petri dish containing molecular-grade sterile water (Sigma-Aldrich, St. Louis, MO). Unattached microbial cells and/or fine-grained glacial till were removed from the mineral phases by gentle agitation of the petri dishes. This process was repeated three times, until no observable till was being released from the mineral phases. Triplicate 500 mg subsamples of individual mineral granules from the coupons were transferred directly to bead-beating DNA extraction vials

**DR 1.5. Community DNA Extraction and Community Bacterial 16S rDNA T-RFLP Analysis.** DNA was extracted from the 500 mg samples of individual mineral substrate, subglacial sediments, and from filter papers in triplicate (duplicate in the case of filtered water) using the Bio101 FastDNA SPIN Kit for Soil (MP Bio Medicals, Solon, OH) using a slightly modified protocol as described previously (Boyd et al., 2007b). Equal volumes of each extraction were pooled and genomic DNA was quantified fluorometrically using previously described methods (Boyd et al., 2007b). Approximately 15 ng of genomic DNA from each substratum type, RG sediment, and RG water filter paper pooled extracts was subjected to thirty cycles of PCR in triplicate using bacterial-specific primers 8F and 907R, according to previously described protocols (Boyd et al., 2007a, however the forward primer was modified with phosphoramidite fluorochrome 5-carboxyfluorescein (FAM) at the

5' terminus (Invitrogen). Replicate PCR products were pooled, purified, and subjected to T-RFLP digestion, electrophoresis, and analysis as previously described {Boyd, 2007 #32}.

**DR 1.6. Statistical Analysis of T-RFLP Electropherograms.** For the purposes of this study, distinct T-RFs were considered to be unique operational taxonomic units (OTU) and were the unit by which individual phylotypes were demarcated. The Bray-Curtis index (e.g., Sørensen index), which represents an abundance weighted metric describing the similarity of communities, ranges from 0 to 1, with higher values indicative of greater similarity. Bray Curtis similarity for community comparisons were calculated using PAST (ver. 1.7.2) (Hammer et al., 2001). Hierarchical cluster analysis with multiple (1000) bootstrap was performed with the program pvclust (<http://www.is.titech.ac.jp/~shimo/prog/pvclust/>) and the base package within R (version 2.10.1) (<http://www.r-project.org/contributors.html>). Hierarchical clustering was based on Ward's agglomerative correlation method with the Bray-Curtis similarity indices serving as input for the analysis.

#### **DR 1.7. PCR Amplification of 16S rRNA Genes for Sequence Analysis.**

Approximately 15 ng of genomic DNA from the subglacial sediment and pyrite substratum DNA extracts was subjected to thirty cycles of PCR in triplicate using bacterial-specific primers 8F and 907R according to previously described protocols (Boyd et al., 2007a). Replicate PCR products were pooled, purified using the Promega Wizard purification kit (Madison, WI), quantified using the Low Mass DNA Ladder (Invitrogen), cloned using the pGEM Easy Vector System (Promega), and sequenced using the M13F and R primer pair as previously described (Boyd et al., 2009). Sequences were assembled using BioEdit (ver.

7.0.9.0) (Hall, 1999) and were checked for chimeric artifacts using Mallard (ver. 1.0.2) (Ashelford et al., 2005).

**DR 1.8. Phylogenetic analysis.** Bacterial 16S rRNA genes from both the subglacial sediment- and pyrite-associated communities were compiled and aligned using ClustalX (ver. 2.0.9) (Thompson et al., 1994) specifying the IUB substitution matrix and default gap extension and opening penalties. The phylogenetic position of bacterial 16S rRNA genes was assessed using PhyML (ver. 3.0) (Guindon and Gascuel, 2003) using the GTR substitution model with gamma-shaped rate variation and a proportion of invariable sites as recommended by ModelTest (ver. 3.8) (Posada, 2006). The 16S rRNA genes from *Acidilobus sulfurireducens* str. 18D70 and *Caldisphaera draconis* str. 18U65, both of which are members of the Crenarchaeota, served as outgroups. The 16S rRNA gene phylogram was rate-smoothed with a molecular clock approach using the multidimensional version of Rambaut's parameterization as implemented in PAUP (ver 4.0) (Swofford, 2001). *P*-values indicating the probability that each environment has more unique branch length (e.g., are not overlapping phylogenetically) than expected by chance were determined using 100 permutations and the weighted Unifrac significance test of each pair of environments as implemented in the program Unifrac (Lozupone and Knight, 2005). If the assemblages did not harbor significant unique branch length at a *P* value of  $< 0.05$ , they were considered to overlap phylogenetically (Lozupone and Knight, 2005).

**DR 1.9. Anions, cations and stable isotopes.** Anion and cation analyses were performed on aliquots of filtered water (0.22  $\mu\text{m}$ ) that were stored on ice in plastic scintillation vials without headspace. Major anions and cations were measured using a Dionex 3000 ICS ion chromatography system (Dionex, Sunnyvale, CA) according to

previously published methods (Lewis et al., 2012). The precision (based on repeats of standards and samples) was better than 2% for all analytes. pH and electrical conductivity were measured in the field by using an Orion 4 Star pH/Conductivity meter and probes designed for low ionic strength solutions. Alkalinity was determined using a Hach Digital Titrator.

The sulfur ( $^{34}\text{S}/^{32}\text{S}$ ) and oxygen ( $^{18}\text{O}/^{16}\text{O}$ ) isotope ratios of  $\text{SO}_4^{2-}$  ( $\delta^{34}\text{S}\text{-SO}_4^{2-}$  and  $\delta^{18}\text{O}\text{-SO}_4^{2-}$ ) were analyzed at the University of Calgary Isotope Lab following standard procedures (University of Calgary, 2010a, b, c). Briefly,  $\text{BaSO}_4$  was precipitated from 1-2L of filtered sample by acidification with HCl and addition of a saturated  $\text{BaCl}_2$  solution (University of Calgary, 2010b). The sulfur isotope ratio of the  $\text{BaSO}_4$  precipitate was measured using Continuous Flow-Isotope Ratio Mass Spectrometry (CF-EA-IRMS) on a Carlo Erba NA 1500 elemental analyzer interfaced to a VG PRISM II mass spectrometer. The sulfur isotope results are expressed in the usual per mil notation ( $\delta^{34}\text{S} \text{ ‰}$ ) relative to the international VCDT standard. The precision of  $\delta^{34}\text{S}_{\text{BaSO}_4}$  using this technique, is generally better than  $\pm 0.25$  (n=10) based on daily reproducibility tests (University of Calgary, 2010c). The  $\delta^{18}\text{O}$  of  $\text{BaSO}_4$  is determined using a high temperature, pyrolysis reactor (Finnigan MAT TC/EA) coupled with an isotope ratio mass spectrometer (Finnigan Mat Delta+XL) in continuous flow mode (using Conflow III open split/interface). Results are expressed in the usual per mil notation ( $\delta^{18}\text{O} \text{ ‰}$ ) relative to the international VSMOW standard. Accuracy and precision of  $\delta^{18}\text{O}$  of  $\text{BaSO}_4$  is generally better than  $\pm 0.3 \text{ ‰}$  (one standard deviation based on n=50 lab standards) (University of Calgary, 2010a). Oxygen ( $^{18}\text{O}/^{16}\text{O}$ ) isotope ratios of  $\text{H}_2\text{O}$  ( $\delta^{18}\text{O}\text{-H}_2\text{O}$ ) were determined using the  $\text{CO}_2\text{-H}_2\text{O}$  equilibrium technique with subsequent analysis using continuous flow input to a ThermoFinnigan DELTAplusXP mass spectrometer (Richardson et al., 2009).  $\delta^{18}\text{O}\text{-H}_2\text{O}$  values are expressed in the usual per mil notation ( $\delta^{18}\text{O} \text{ ‰}$ ) relative to the international VSMOW standard.

## DR 2. EXTENDED RESULTS

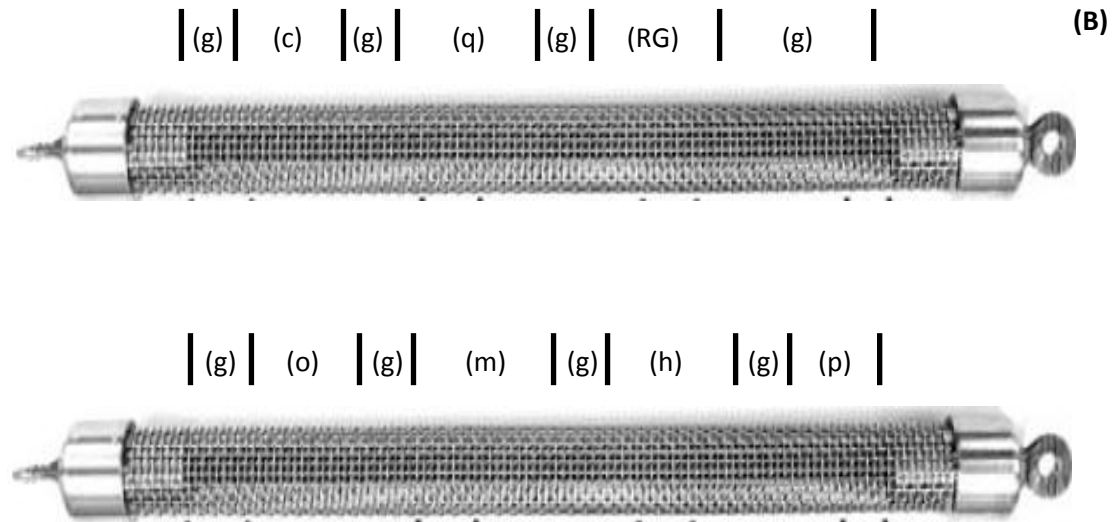
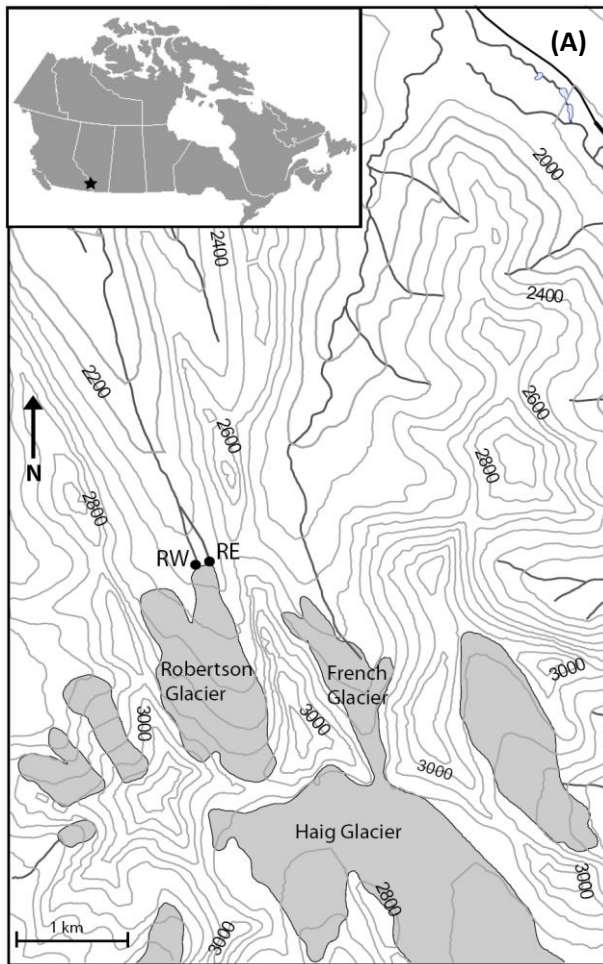


Fig DR1. (A) Topographic map of RG showing the two bulk meltwater streams RW and RE. The coupons were incubated ~ 10m from the snout of the glacier in RW. Gray shaded areas are glaciers. Contour interval is 100 m. The inset image (top left) indicates the location of RG (star) within Alberta, Canada. Map was prepared from NTS 1:50,000 maps 82J/14 and 82J/11 (© Department of Natural Resources Canada. All rights reserved). (B) Biofilm coupon ( $25.4 \times 1.27$  cm) used to retain mineral phases during incubation in subglacial environment. Two coupons were required to contain all the mineral phases. These were located in each, as shown above. Glass wool spacer (g), pyrite (p), hematite (h), magnetite (m), quartz (q), calcite (c), olivine (o), catchment rock (RG).



Table DR1. Mineralogical (X-Ray Diffraction [XRD]) and elemental composition (Energy-dispersive X-ray spectroscopy [EDS]) of a selection of catchment rocks, and proglacial sediment from the Robertson catchment. Elemental composition of minerals used in incubated coupons also shown. Main rocks types observed and collected were limestone (with impurities) and shale. \* Indicates rock which was crushed and used in mineral coupons (RG Rock). General rock types: Silty limestone (SL); Argillaceous limestone (AL); Dark Shale (S).

Catchment Rocks							
Mineral	Formula	R1	R2	R3	R4	R5*	RG Sediment
Calcite	CaCO <sub>3</sub>	✓	✓	✓	✓	✓	✓
Quartz	SiO <sub>2</sub>	✓	✓	✓	✓	✓	✓
Pyrite	FeS <sub>2</sub>	✓		✓		✓	✓
Microcline	KAlSi <sub>3</sub> O <sub>8</sub>		✓				✓
Montmorillonite-14A	Na <sub>0.3</sub> (Al,Mg) <sub>2</sub> Si <sub>4</sub> O <sub>10</sub> (OH) <sub>2</sub> H <sub>2</sub> O		✓				
Montmorillonite-18A	Na <sub>0.3</sub> (Al Mg) <sub>2</sub> Si <sub>4</sub> O <sub>10</sub> OH <sub>2</sub> 6H <sub>2</sub> O		✓				
Muscovite	KAl <sub>2</sub> Si <sub>3</sub> AlO <sub>10</sub> (OH) <sub>2</sub>			✓		✓	
Nontronite-15A	Na <sub>0.3</sub> Fe <sub>2</sub> Si <sub>4</sub> O <sub>10</sub> (OH) <sub>2</sub> 4H <sub>2</sub> O	✓					
Sanidine	K(Si <sub>3</sub> Al)O <sub>8</sub>				✓	✓	
Ankerite	Ca(Fe,Mg)(CO <sub>3</sub> ) <sub>2</sub>			✓			
Element	(weight %) by EDS	Coupon minerals					
		Oli-vine	Pyrite	Hem-atite	Mag-netite	Cal-cite	Qua-rtz
O	55	46		30	16	48	70
Na	nd						
Mg	0.71						
Al	1.1						
Si	5.8						30
S	0.79		53				
K	0.58						
Ca	36					40	
Fe	0.89	7.5	47	70	84		
Cr	nd	0.36					
Ni	nd	0.49					

Table DR2. Meltwater chemistry from the supraglacial and subglacial (bulk meltwater) environment at RG. Units, dissolved ions, in  $\mu$  moles  $L^{-1}$ . Enrichment factors shown are calculated as the ratio of the average concentration of species in the July supraglacial meltwater relative to concentrations in RW bulk meltwater in July (17/07/2007) and on coupon installation day in October (13/10/2007). See section DR2.1 and 2.2 for extended description.

	Supraglacial (17/7/2007)				Subglacial / bulk meltwaters (RW) (17/7/2007)				Subglacial / bulk meltwaters (RW) (13/10/2007)	Enrichment factor (17/7/2007)	Enrichment factor (13/10/2007)
Time	min	max	Average (n=5)	var%	min	max	Average (n=2)	var%	n = 1		
EC ( $\mu S/cm$ )	3.5	27	11	84	79	87	83	7.1	460	7.6	42
pH	6.8	8.6	7.7	8.2	7.2	7.4	7.3	1.3	6.8	0.95	0.89
Cl <sup>-</sup>	0.17	0.99	0.54	66	0.48	2.3	1.4	92	8.5	2.6	16
SO <sub>4</sub> <sup>2-</sup>	0.36	0.91	0.58	37	110	160	140	21	2100	230	3600
NO <sub>3</sub> <sup>-</sup>	0	1.2	0.63	81	1.6	3.4	2.6	47	1.3	4.0	2.1
Na <sup>+</sup>	0.20	1.4	0.78	76	1.9	3.4	2.6	41	44	3.3	55
NH <sub>4</sub> <sup>+</sup>	0.17	1.7	0.72	94	1.2	1.3	1.3	2.6	0.67	1.7	0.91
K <sup>+</sup>	0.049	1.2	0.36	120	2.0	2.8	2.3	23	28	6.4	77
Mg <sup>2+</sup>	1.5	4.0	2.3	43	44	60	52	21	990	22	41
Ca <sup>2+</sup>	15	140	57	92	270	270	270	1.1	2200	4.8	40
Measured HCO <sub>3</sub> <sup>-</sup>	43	260	120	74	390	410	390	1.7	1500	3.3	13
$\delta^{34}S-SO_4^{2-}$	-	-	-	-	-	-	-	-	3.0	-	-
$\delta^{18}O-SO_4^{2-}$	-	-	-	-	-	-	-	-	-13.2	-	-
$\delta^{18}O-H_2O$	-	-	-	-	-19.1	-19.2	-19.2	0.50%	-18.7	-	-

Table DR3. Phylogenetic affiliation of phylotypes associated with 16S rRNA gene clone libraries from DNA extracted from (a) pyrite and (b) RG sediment. See section DR2.3 for extended description. Organisms that have been demonstrated to catalyze the oxidation of soluble and/or solid phase ferrous iron and sulfur in pure cultures (Karavaiko et al., 2003; Okereke and Stevens, 1991; Susuki et al., 1990) are shown in comments.

97% similarity threshold for OTU clustering

Clone (Accession#)	Freq	Closest BLAST Hit (Accession #) (% identity)	Closest Cultivated Organism (Accession #) (% identity)	Class	Comments
<b>(a) PYRITE</b>					
P1 (HM635783)	5	Uncultured glacial foreground soil bacterium clone (GQ397041) (98%)	<i>Steroidobacter denitrificans</i> strain FS (EF605262) (88%)	$\gamma$ -Proteobacteria	
P3 (HM635784)	1	Uncultured marine sediment bacterium clone (EF459825) (97%)	<i>Demequina lutea</i> strain SV47 (79%)	Actinobacteria	
P4 (HM635785)	1	Uncultured marine bacterium clone (EU803726) (97%)	<i>Ilumatobacter fluminis</i> (AB360343) (88%)	Actinobacteria	
P5 (HM635786)	3	Uncultured freshwater sediment bacterium clone (DQ463271) (98%)	<i>Flavobacterium granuli</i> (AB180738) (96%)	Flavobacteria	
P9 (HM635787)	1	Flavobacterium sp. FB7 (AM933500) (96%)	Flavobacterium columnare (AY747592) (96%)	Flavobacteria	
P16 (HM635788)	1	Uncultured glacial foreground soil bacterium clone (GQ396822) (99%)	<i>Thiobacillus denitrificans</i> strain ME16 (EU546130) (94%)	$\beta$ -Proteobacteria	iron/sulfur cycling
P18 (HM635789)	2	Uncultured high arctic desert bacterium clone (AM940601) (96%)	<i>Sporocytophaga</i> sp. 4v (FJ372724) (85%)	Cytophagia	
P19 (HM635790)	6	<i>Clostridium pasteurianum</i> (M23930) (99%)	<i>Clostridium pasteurianum</i> (M23930) (99%)	Clostridia	
P20 (HM635791)	1	Uncultured glacial sediment clone 39B (EU919774) (94%)	<i>Thiobacillus denitrificans</i> strain ME16 (EU546130) (94%)	$\beta$ -Proteobacteria	iron/sulfur cycling
P21 (HM635792)	1	Uncultured wastewater clone (AB305033) (96%)	<i>Caldilinea aerophila</i> (AB067647) (87%)	Caldilineae	
P22 (HM635793)	1	Uncultured glacial sediment clone 39B (EU919774) (95%)	<i>Thiobacillus thiophilus</i> strain D24TN (EU685841) (94%)	$\beta$ -Proteobacteria	iron/sulfur cycling
P23 (HM635794)	1	Uncultured gold mine bacterium (AF337875.2) (98%)	<i>Acidithiobacillus ferrooxidans</i> (AJ459800) (90%)	$\gamma$ -Proteobacteria	iron/sulfur cycling
P26 (HM635795)	4	Uncultured Svalbardsoil clone (EU919753) (99%)	<i>Thiobacillus denitrificans</i> strain ME16 (EU546130) (97%)	$\beta$ -Proteobacteria	iron/sulfur cycling
P29 (HM635796)	1	Uncultured Subglacial clone (DQ628916) (95%)	<i>Pseudorhodobacter incheonensis</i> strain KOPRI (DQ001322) (94%)	$\alpha$ -Proteobacteria	
P30 (HM635797)	1	Uncultured gold mine bacterium (AF337868.2) (94%)	<i>Nitrosospira multiformis</i> ATCC 25196 (CP000103) (93%)	$\beta$ -Proteobacteria	
P32 (HM635798)	1	Uncultured cave clone (DQ823151) (98%)	<i>Sphingomonas jaspis</i> (AB264131) (97%)	$\alpha$ -Proteobacteria	
P36 (HM635799)	1	Uncultured gold mine bacterium (AF337875.2) (98%)	<i>Acidithiobacillus ferrooxidans</i> (AJ459800) (90%)	$\gamma$ -Proteobacteria	iron/sulfur cycling
P38 (HM635800)	1	Uncultured freshwater clone (EU117950) (99%)	<i>Terracoccus luteus</i> strain DSM 44267 (NR_026412) (89%)	Actinobacteria	
P42 (HM635801)	1	Uncultured Antarctic sub ice clone (DQ521467) (99%)	<i>Brevundimonas</i> sp. AKB-2008-JO103 (AM988997) (99%)	$\alpha$ -Proteobacteria	
P44 (HM635802)	1	Uncultured aquifer clone (EU735705) (97%)	<i>Thiobacillus denitrificans</i> strain ME16 (EU546130) (92%)	$\beta$ -Proteobacteria	iron/sulfur cycling
P47 (HM635803)	1	Uncultured subglacial clone (DQ228359) (98%)	<i>Siderooxidans lithoautotrophicus</i> strain ES-1 (DQ386264) (95%)	$\gamma$ -Proteobacteria	iron/sulfur cycling
P48 (HM635804)	1	Uncultured dust bacterium (FM874454) (96%)	<i>Arenimonas</i> sp. YC6267 (EU376961) (94%)	$\gamma$ -Proteobacteria	
<b>(b) RG SEDIMENT</b>					
S3 (HM635805)	10	Uncultured subglacial sediment bacterium clone (DQ228359) (91%)	<i>Siderooxidans lithoautotrophicus</i> str. ES-1 (DQ386264) (96%)	$\gamma$ -Proteobacteria	iron/sulfur cycling
S5 (HM635806)	1	Uncultured subglacial sediment bacterium clone (DQ228359) (99%)	<i>Rhodoferrax ferrireducens</i> T118 (CP000267) (98%)	$\beta$ -Proteobacteria	iron/sulfur cycling
S9 (HM635807)	3	Uncultured glacial sediment bacterium clone (EU919753) (99%)	<i>Thiobacillus denitrificans</i> str. ME16 (EU546130) (97%)	$\beta$ -Proteobacteria	iron/sulfur cycling
S11 (HM635808)	2	Uncultured freshwater bacterium clone (FJ694303) (98%)	<i>Flavobacterium</i> sp. SOC A4(12) (DQ628951) (97%)	Flavobacteria	
S15 (HM635809)	1	Uncultured aquatic bacterium clone (EU800906) (98%)	<i>Paucimonas lemoignei</i> (X92554) (91%)	$\beta$ -Proteobacteria	
S22 (HM635810)	2	Uncultured subglacial sediment bacterium clone (AF479323) (97%)	<i>Rhodoglobus</i> sp. 01WB01-49 (FM161352) (97%)	Actinobacteria	
S26 (HM635811)	1	Uncultured glacial ice bacterium clone (EU978700) (100%)	<i>Brevundimonas</i> sp. 39(2008) (FJ197848) (98%)	$\alpha$ -Proteobacteria	
S27 (HM635812)	3	Uncultured glacial foreground soil bacterium clone (GQ397041) (97%)	<i>Beggiatoa</i> sp. 402 (AY583996) (91%)	$\gamma$ -Proteobacteria	
S34 (HM635813)	1	Uncultured Antarctica freshwater bacterium clone (EU869545) (99%)	<i>Rhodobacter</i> sp. ZS5-10 (FJ196040) (99%)	$\alpha$ -Proteobacteria	
S35 (HM635814)	1	Uncultured microbial mat clone (GQ441301) (98%)	<i>Kryptoperidinium foliaceum</i> strain CCMP1326 (GU591328)	Dinophyceae	
S39 (HM635815)	1	Uncultured glacial foreground soil bacterium clone (GQ397021) (94%)	<i>Sideroxydans lithotrophicus</i> ES-1 (CP001965) (90%)	$\beta$ -Proteobacteria	iron/sulfur cycling
S40 (HM635816)	1	Uncultured glacial sediment bacterium clone (DQ228387) (97%)	<i>Thiobacillus denitrificans</i> str. ME16 (EU546130) (94%)	$\beta$ -Proteobacteria	iron/sulfur cycling
S46 (HM635817)	3	Uncultured subglacial sediment bacterium clone (DQ228367) (95%)	<i>Siderooxidans lithoautotrophicus</i> str. ES-1 (DQ386264) (93%)	$\gamma$ -Proteobacteria	iron/sulfur cycling
S47 (HM635818)	1	Uncultured glacial foreground soil bacterium clone (GQ397041) (98%)	<i>Steroidobacter denitrificans</i> str. FS (EF605262) (88%)	$\gamma$ -Proteobacteria	
S48 (HM635819)	1	Uncultured aquifer sediment bacterium clone (EU266776) (97%)	<i>Candidatus Magnetobacterium bavaricum</i> (FP929063) (87%)	<i>Nitrospira</i>	

Table DR4. Relative abundance<sup>a,b</sup> of T-RFs recovered from filtered water (RG water), RG sediment, or coupon rock- (RG rock) and mineral-associated bacterial communities.

T-RF (bp) <sup>c</sup>	RG Water	RG Sediment	Pyrite	Calcite	Magnetite	Hematite	RG Rock	Olivine	Quartz
67.9								3.3 (0.2)	
80.6		16.5 (5.6)	3.0 (1.1)	7.1 (3.6)	7.5 (0.5)	5.3 (1.6)			7.5 (0.6)
94.9								3.1 (0.4)	
117.5								13.2 (1.1)	
118.6	15.2 (1.0)	2.6 (0.5)	4.5 (1.4)				6.6 (0.7)	5.0 (0.3)	
120.5		11.4 (1.7)			3.2 (0.5)		2.5 (0.2)		
134.6	4.7 (0.2)	3.1 (0.7)					8.8 (0.7)		
136.6	4.6 (0.2)	3.2 (0.4)		2.8 (0.3)	3.3 (0.7)			11.8 (0.9)	
138.7	3.0 (0.2)			3.6 (0.3)	7.7 (0.4)		3.3 (0.3)	2.7 (0.3)	
141.1						4.7 (1.2)			
144.9		4.5 (0.7)					3.1 (0.4)		25.0 (0.8)
147.4	3.0 (0.1)	5.6 (1.7)			4.8 (1.2)			2.9 (0.1)	
150.3					3.6 (1.0)				
161.6								5.1 (0.4)	
176.9									25.2 (0.6)
206.7					4.5 (0.4)				
268.2								5.0 (0.2)	
282.3								2.8 (0.5)	
292.8								2.8 (0.1)	
294.6								2.9 (0.3)	3.5 (0.0)
297.9								4.6 (0.1)	4.5 (0.1)
401.4			2.9 (0.4)		4.8 (1.3)	7.0 (1.8)			5.8 (0.2)
402.7									4.4 (0.2)
427.6		5.7 (1.4)							
429.4	5.4 (0.2)	9.4 (1.2)	9.7 (0.8)				15.5 (0.6)		
430.9	11.5 (0.5)	3.0 (1.3)	11.1 (1.0)				14.4 (0.7)		4.3 (0.3)
433.0		3.8 (1.3)	7.2 (0.7)						

436.9					3.3 (0.6)	3.7 (0.8)			
439.3		5.0 (1.6)							
456.8						3.2 (0.8)	3.8 (0.3)		7.2 (0.5)
460.6						3.4 (1.0)			
468.3					3.9 (0.7)				
477.6			2.5 (0.2)						
482.2				3.1 (0.9)				18.9 (1.4)	
485.7	9.6 (0.6)	7.4 (3.8)	3.0 (0.2)	5.3 (1.5)	13.8 (2.4)	15.3 (3.2)	2.6 (0.2)		
488.7						5.8 (5.1)			
489.8	40.2 (0.7)	3.9 (2.0)	8.6 (1.6)	12.8 (3.7)	15.9 (8.5)	7.1 (5.2)	13.4 (3.5)		
492.4	2.8 (0.2)	7.4 (1.9)	7.2 (1.3)			5.8 (5.1)	3.2 (0.3)	3.1 (0.4)	4.1 (0.2)
494.6		3.9 (1.4)	9.3 (0.4)				15.2 (1.1)		
498.6						6.6 (1.6)			
499.7						3.2 (0.8)			
502.1						3.1 (0.8)			
511.8			13.9 (0.7)	45.0 (9.4)					
531.5						8.9 (2.4)			
534.7			3.3 (0.3)	3.0 (0.9)	5.3 (1.4)	3.8 (0.9)			
539.6						8.6 (2.6)			
542.0					11.3 (1.5)		4.3 (0.4)		8.5 (0.8)
559.2								3.3 (0.4)	
570.6			6.5 (0.6)	8.0 (2.4)					
600.7			4.0 (0.3)		3.3 (0.5)		3.4 (0.2)		
605.5				2.7 (0.7)				5.8 (0.8)	
688.2		3.6 (1.4)			3.6 (0.4)	4.6 (1.6)			
872.0								3.7 (0.6)	
887.5			3.1 (0.2)	6.4 (1.9)					
Total	100.0	100.0	100.0	100.0	100.0	100.0	100.0	100.0	100.0

<sup>a</sup>Percent of total fluorescence (TF) of phylotypes representing greater than 2.0% TF. <sup>b</sup>Standard deviations of three replicate profiles reported in parentheses. <sup>c</sup>Terminal restriction fragment (T-RF) as base-pair (bp) length.

Table DR5. Bray–Curtis similarity of bacterial 16S rRNA gene assemblages derived from T-RFs (Table DR4) associated with different mineral substrata, Robertson Glacier (RG) sediments, or RG meltwater (RG Water).

<b>Bray-Curtis</b>	<i>RG Water</i>	<i>Sediment</i>	<i>Pyrite</i>	<i>Calcite</i>	<i>Magnetite</i>	<i>Hematite</i>	<i>RG Rock</i>	<i>Olivine</i>	<i>Quartz</i>
<i>RG Water</i>	1.00	0.34	0.35	0.24	0.35	0.19	0.50	0.18	0.07
<i>Sediment</i>		1.00	0.40	0.19	0.34	0.26	0.37	0.12	0.19
<i>Pyrite</i>			1.00	0.41	0.24	0.25	0.52	0.08	0.14
<i>Calcite</i>				1.00	0.35	0.21	0.19	0.11	0.07
<i>Magnetite</i>					1.00	0.42	0.29	0.09	0.21
<i>Hematite</i>						1.00	0.16	0.03	0.18
<i>RG Rock</i>							1.00	0.11	0.19
<i>Olivine</i>								1.00	0.11
<i>Quartz</i>									1.00

**DR 2.1. Meltwater chemistry.** Meltwaters collected from the supraglacial environment were dilute, with an average  $EC = 11 \mu S cm^{-1}$ . Conversely, subglacial meltwaters collected at the site of coupon deployment in RW stream, were more concentrated than supraglacial waters by 7 times on average in July 2007 ( $EC = 83 \mu S cm^{-1}$ ) and 42 times in October 2007 ( $EC = 460 \mu S cm^{-1}$ ) when the coupons were deployed. The dominant cation in the subglacial meltwaters was  $Ca^{2+}$  (average, July =  $270 \mu M L^{-1}$ ) and the dominant anion was typically bicarbonate (average, July =  $390 \mu M L^{-1}$ ), followed by  $SO_4^{2-}$  (average, July =  $140 \mu M L^{-1}$  (Table DR2). Although, at the time of deployment  $SO_4^{2-}$  concentration ( $2100 \mu M L^{-1}$ ) exceeded bicarbonate ( $1500 \mu M L^{-1}$ ). The enrichment of individual ions from the supraglacial to subglacial environment was greatest for  $SO_4^{2-}$  (230 to 3600 times enriched),  $Na^+$  (3 to 55 times enriched),  $K^+$  (6 to 77 times enriched),  $Mg^{2+}$  (22 to 41 times enriched) and  $Ca^{2+}$  (5 to 40 times enriched), with the greatest enrichment in October when subglacial meltwaters were most concentrated. Conversely,  $NH_4^+$  and  $NO_3^-$  were less enriched in subglacial meltwaters in October, with greatest enrichment in July (Boyd et al., 2011). The pH of the subglacial meltwaters was neutral to mildly basic, ranging between 6.8 and 7.4.

**DR 2.2. Isotope Geochemistry**  $\delta^{34}S$ - $SO_4^{2-}$  and  $\delta^{18}O$ - $SO_4^{2-}$  values from RW at the time of the coupon deployment suggest pyrite as the dominant  $SO_4^{2-}$  source (Table DR2). The  $\delta^{34}S$  values from pyrite are usually slightly positive (e.g. 0 to 10‰), although reported values vary widely (-20 to 15‰, (Nielsen et al., 1991)). However, the  $\delta^{34}S$  values of sulfate in Upper Devonian evaporites in North America are very positive, with  $\delta^{34}S$  values ranging from approximately 22 to 34‰ (Nielsen et al., 1991). Thus, the  $\delta^{34}S$  value of sulfate in RW at 3 ‰ is consistent with a pyrite rather than evaporite source. Further, the  $\delta^{18}O$  value of sulfate in Upper

Devonian evaporites in North America varies between approximately 13 to 18‰ (Nielsen et al., 1991) while, the  $\delta^{18}\text{O}\text{-SO}_4^{2-}$  values in the RW sample is negative (-13‰). A plausible process that could account for the negative  $\delta^{18}\text{O}\text{-SO}_4^{2-}$  value is that a portion of the  $\text{SO}_4^{2-}$  was produced via anoxic sulfide oxidation, a process where most or all of the oxygen in  $\text{SO}_4^{2-}$  are derived from the water ( $\delta^{18}\text{O}\text{-H}_2\text{O}$ , -18.7 ‰) (Bottrell and Tranter, 2002; Lafrenière and Sharp, 2005).

**DR 2.3. Bacterial Community Composition.** To characterize the influence of pyrite on subglacial sediment-associated bacterial community composition, we characterized the diversity of 16S rRNA genes recovered from pyrite-associated minerals, as well as from native subglacial sediments sampled adjacent to the mineral coupons (main paper, Figure 1; Table DR3). A large proportion of the clones were most closely affiliated with lithotrophic organisms that metabolize Fe and /or S, (main paper, Figure 1; Table DR3). For example, 56% of the 16S rRNA gene clones recovered from the sediment-associated community were most closely affiliated with *Sideroxydans lithotrophicus* ES-1 and *Thiobacillus denitrificans* ME16, both of which have been shown to oxidize ferrous iron in pure culture (Emerson et al., 2007; Karavaiko et al., 2003; Okereke and Stevens, 1991; Suzuki et al., 1990). Additionally the closest BLAST hits for 46% of the pyrite-associated clones and 84% of the sediment-associated clones were from uncultured microorganisms recovered from other glacial or polar soils and subglacial sediments (Table DR3). This finding is consistent with the proposal that glacierised environments are selecting for similar communities, due to mineralogical controls imparted by similar bedrock geology (Skidmore et al., 2005), in concert with prevailing hydrological regimes (Tranter et al., 2005), nutrient availability and redox conditions (Wadham et al., 2004; Wynn et al., 2007).



## References.

- Ashelford, K.E., Chuzhanova, N.A., Fry, J.C., Jones, A.J., and Weightman, A.J., 2005, At Least 1 in 20 16S rRNA Sequence Records Currently Held in Public Repositories Is Estimated To Contain Substantial Anomalies: Applied and Environmental Microbiology, v. 71, p. 7724-7736.
- Bottrell, S.H., and Tranter, M., 2002, Sulphide oxidation under partially anoxic conditions at the bed of the Haut Glacier d'Arolla, Switzerland: Hydrological Processes, v. 16, p. 2363-2368.
- Boyd, E., Cummings, D., and Geesey, G., 2007a, Mineralogy Influences Structure and Diversity of Bacterial Communities Associated with Geological Substrata in a Pristine Aquifer: Microbial Ecology, v. 54, p. 170-182.
- Boyd, E.S., Jackson, R.A., Encarnacion, G., Zahn, J.A., Beard, T., Leavitt, W.D., Pi, Y., Zhang, C.L., Pearson, A., and Geesey, G.G., 2007b, Isolation, Characterization, and Ecology of Sulfur-Respiring Crenarchaea Inhabiting Acid-Sulfate-Chloride-Containing Geothermal Springs in Yellowstone National Park: Applied and Environmental Microbiology, v. 73, p. 6669-6677.
- Boyd, E.S., King, S., Tomberlin, J.K., Nordstrom, D.K., Krabbenhoft, D.P., Barkay, T., and Geesey, G.G., 2009, Methylmercury enters an aquatic food web through acidophilic microbial mats in Yellowstone National Park, Wyoming: Environmental Microbiology, v. 11, p. 950-959.
- Boyd, E.S., Lange, R.K., Mitchell, A.C., Havig, J.R., Hamilton, T.L., Lafrenière, M.J., Shock, E.L., Peters, J.W., and Skidmore, M., 2011, Diversity, Abundance, and Potential Activity of Nitrifying and Nitrate-Reducing Microbial Assemblages in a

- Subglacial Ecosystem: *Applied and Environmental Microbiology*, v. 77, p. 4778-4787.
- Emerson, D., Rentz, J.A., Lilburn, T.G., Davis, R.E., Aldrich, H., Chan, C., and Moyer, C.L., 2007, A Novel Lineage of Proteobacteria Involved in Formation of Marine Fe-Oxidizing Microbial Mat Communities: *PLoS ONE*, v. 2, p. e667.
- Guindon, S., and Gascuel, O., 2003, A Simple, Fast, and Accurate Algorithm to Estimate Large Phylogenies by Maximum Likelihood: *Systematic Biology*, v. 52, p. 696-704.
- Hall, T.A., 1999, BioEdit: a user-friendly biological sequence alignment editor and analysis program for Windows 95/98/NT: *Nucleic Acids Symposium Series*, v. 41, p. 95-98.
- Hammer, Ø., Harper, D.A.T., and Ryan, P.D., 2001, PAST: paleontological statistics software package for education and data analysis. : *Palaeontol. Electronica*.
- Karavaiko, G.I., Turova, T.P., Kondrat'eva, T.F., Lysenko, A.M., Kolganova, T.V., Ageeva, S.N., Muntyan, L.N., and Pivovarova, T.A., 2003, Phylogenetic heterogeneity of the species *Acidithiobacillus ferrooxidans*: *International Journal of Systematic and Evolutionary Microbiology*, v. 53, p. 113–119, doi:10.1099/ijs.0.02319-0.
- Lafrenière, M.J., and Sharp, M.J., 2005, A comparison of solute fluxes and sources from glacial and non-glacial catchments over contrasting melt seasons: *Hydrological Processes*, v. 19, p. 2991-3012.
- Lewis, T., Lafrenière, M.J., and Lamoureux, S.F., 2012, Hydrochemical and sedimentary responses of paired High Arctic watersheds to unusual climate and permafrost disturbance, Cape Bounty, Melville Island, Canada: *Hydrological Processes*, v. 26, p. 2003-2018.
- Lozupone, C., and Knight, R., 2005, UniFrac: a New Phylogenetic Method for Comparing Microbial Communities: *Appl. Environ. Microbiol.*, v. 71, p. 8228-8235.

- McMechan, M.E., 1988, Geology of Peter Lougheed Provincial Park, Rocky Mountain Front Ranges, Alberta. : Open File Report 2057, Geological Survey of Canada.
- Nielsen, H., Pilot, J., Grinenko, L., Grinenko, V., Lein, A., Smith, J., and and Pankina, R., 1991, Lithospheric Sources of Sulfur, *in* Krouse, H., and Grinenko, V., eds., Stable Isotopes: Natural and Anthropogenic Sulphur in the Environment, John Wiley and Sons, p. 65-132.
- Okereke, A., and Stevens, S.E., Jr., 1991, Kinetics of Iron Oxidation by *Thiobacillus ferrooxidans*: Applied and Environmental Microbiology , v. 57, p. 1052-1056.
- Posada, D., 2006, ModelTest Server: a web-based tool for the statistical selection of models of nucleotide substitution online: Nucleic Acids Research, v. 34, p. W700-W703.
- Richardson, L.E., Kyser, T.K., James, N.P., and Bone, Y., 2009, Analysis of hydrographic and stable isotope data to determine water masses, circulation, and mixing in the eastern Great Australian Bight: Journal of Geophysical Research, v. 114. pages?
- Sharp, M., Creaser, R.A., and Skidmore, M., 2002, Strontium isotope composition of runoff from a glaciated carbonate terrain: Geochimica et Cosmochimica Acta, v. 66, p. 595-614.
- Skidmore, M., Anderson, S.P., Sharp, M., Foght, J., and Lanoil, B.D., 2005, Comparison of Microbial Community Compositions of Two Subglacial Environments Reveals a Possible Role for Microbes in Chemical Weathering Processes: Applied and Environmental Microbiology, v. 71, p. 6986-6997.
- Suzuki, I., Takeuchi, T.L., Yuthasastrakosol, T.D., and Oh, J.K., 1990, Ferrous Iron and Sulfur Oxidation and Ferric Iron Reduction Activities of *Thiobacillus ferrooxidans* Are Affected by Growth on Ferrous Iron, Sulfur, or a Sulfide Ore: Applied and Environmental Microbiology, v. 56, p. 1620-1626.

- Swofford, D.L., 2001, Paup: phylogenetic analysis using parsimony (and other methods), 4.0b10 ed.: Sunderland, Massachusetts., Sinauer Associate.
- Tranter, M., Skidmore, M., and Wadham, J., 2005, Hydrological controls on microbial communities in subglacial environments: Hydrological Processes, v. 19, p. 995-998.
- Thompson, J.D., Higgins, D.G., and Gibson, T.J., 1994, CLUSTAL W: improving the sensitivity of progressive multiple sequence alignment through sequence weighting, position-specific gap penalties and weight matrix choice: Nucleic Acids Research, v. 22, p. 4673-4680.
- University of Calgary, I., 2010a,  $^{18}/^{16}\text{O}$  of solids by CF-TCEA-IRMS <http://www.ucalgary.ca/uofcisl/node/5>, April 7, 2010.
- , 2010b, Precipitation of  $\text{BaSO}_4$  for  $\delta^{34}\text{S}$  analysis, <http://www.ucalgary.ca/uofcisl/node/5>, April 7, 2010.
- , 2010c, Sulfur isotope analyses by continuous-flow isotope ratio mass spectrometry, <http://www.ucalgary.ca/uofcisl/node/5>, April 7, 2010.
- Wadham, J.L., Bottrell, S., Tranter, M., and Raiswell, R., 2004, Stable isotope evidence for microbial sulphate reduction at the bed of a polythermal high Arctic glacier: Earth and Planetary Science Letters, v. 219, p. 341–355, doi:10.1016/S0012-821X(03)00683-6.
- Wynn, P.M., Hodson, A.J., Heaton, T.H.E., and Chenery, S.R., 2007, Nitrate production beneath a High Arctic glacier, Svalbard: Chemical Geology, v. 244, p. 88-102.